Published in : Polymer Chemistry (2018), vol. 9, issue 19, pp. 2650-2659
doi.org/10.1039/c8py00281a
Status : Postprint (Author's version)

BIO-BASED POLY(HYDROXYURETHANE) GLUES FOR METAL SUBSTRATES

Satyannarayana Panchireddy, Bruno Grignard, Jean-Michel Thomassin, Christine Jerome and Christophe Detrembleur *

**Center for Education and Research on Macromolecules (CERM), CESAM Research Unit, University of Liège, allée du 6 août, Building B6A, Agora Square, 4000 Liège, Belgium. E-mail: christophe.detrembleur@uliege.be; Tel: +32 43663465*

† Electronic supplementary information (ESI) available. See DOI: 10.1039/ c8py00281a

Abstract

Bio- and CO_2-based high performance thermoset poly(hydroxyurethane) (PHU) glues were designed from solvent- and isocyanate-free formulations based on cyclocarbonated soybean oil, diamines (aliphatic, cycloaliphatic or aromatic) and functional silica or ZnO fillers. Shear strength values and cohesive or adhesive failure of glues were correlated with the crosslinking, mechanical and thermal properties of the nanocomposite PHU thermosets. The addition of SiO_2 or ZnO fillers bearing cyclic carbonate groups at their surface enabled strong improvement in the adhesion performances of the glues up to 173% compared to the unfilled PHUs. The most performing reinforced PHU adhesives showed a shear strength up to 11.3 MPa for an aluminum substrate, and 10.1 MPa for stainless steel with cohesive failure. This study highlights that bio-based nanocomposite PHU thermosets are promising sustainable alternatives to conventional glues made of toxic formulations containing isocyanates.

Introduction

Glues play a vital role in a wide range of industrial applications, including post-it notes, packaging, automotive, airplane assemblies, etc. Due to their intrinsic and tunable properties such as flexibility, abrasion and chemical resistance, thermal stability and good mechanical performances, polyurethane (PU) materials are widely valorised as coatings, foams, elastomers and also as adhesives.[1–6] They are produced by the polyaddition of polyisocyanates[7,8] with diols, but present some limitations such as the involvement of toxic monomers (isocyanates) that are harmful to human health.[9] In contrast, PU research studies focus now on the development of greener routes for their synthesis by the polyaddition of (activated) five-membered biscyclic carbonates with diamines.[10–37] The resulting poly(hydroxyurethane)s (PHUs) structurally differ from conventional PUs by the presence in the β-position of the urethane bond of primary and/or secondary alcohols.[30,38,39] Inspired by the presence of these pendant hydroxyl groups throughout the polymer, our attention shifted to designing materials as high-performance novel glues that may compete with the traditional PU ones by favouring the adhesive/substrate interactions via hydrogen bonding. Leitsch et al.[40] reported on PU/PHU hybrid adhesives produced by curing low molar mass cyclic carbonates and functional α,ω-telechelic isocyanate-based PU prepolymers with polyamines. The resulting hybrid materials showed good adhesion onto polyimide, poly (vinyl chloride) and aluminum. Additionally,

Published in : Polymer Chemistry (2018), vol. 9, issue 19, pp. 2650-2659
doi.org/10.1039/c8py00281a
Status : Postprint (Author's version)

these hybrid polymers predominantly underwent cohesive failure, a key characteristic for developing high performance adhesives. The first solvent-free and isocyanate-free PU adhesives for wood, glass and epoxy painted aluminum supports were reported in 2016 by Cornille et al.[41] The bonded adhesives were cured at 80 °C for 12 h and 150 °C for 30 min, and cohesive failure was observed for PHU (TMPTC/EDR-148) glues on epoxy painted aluminum (shear strength ≈ 3 MPa). Recently, our group designed novel thermoset reinforced PHU glues for bare aluminum with excellent adhesive performances.[42] Solventfree multifunctional cyclic carbonate/diamine formulations were added with 5 wt% of cyclic carbonate functional ZnO fillers. These fillers significantly improved the crosslinking, the thermal stability, the mechanical properties and also the adhesion performances of PHUs. However, the presence of hydroxyl groups along the polymer backbone rendered the PHUs hydrophilic that favoured adhesive delamination when the surface was immersed in water. This limitation was overcome by incorporating hydrophobic PDMS segments within the PHU formulations, which provides high performance PHU glues for Al substrates with shear strength up to 16.3 MPa. However, water uptake was still between 36 and 50 wt% for the best formulations that might limit the applicability of the process, for instance, when the metal substrate has also to be protected from corrosion. Current challenges are to provide high performance environmentally friendly PHU glues with low water absorption, ideally from bio-resourced starting materials (vegetable oils for instance) and by using solvent-free formulations.

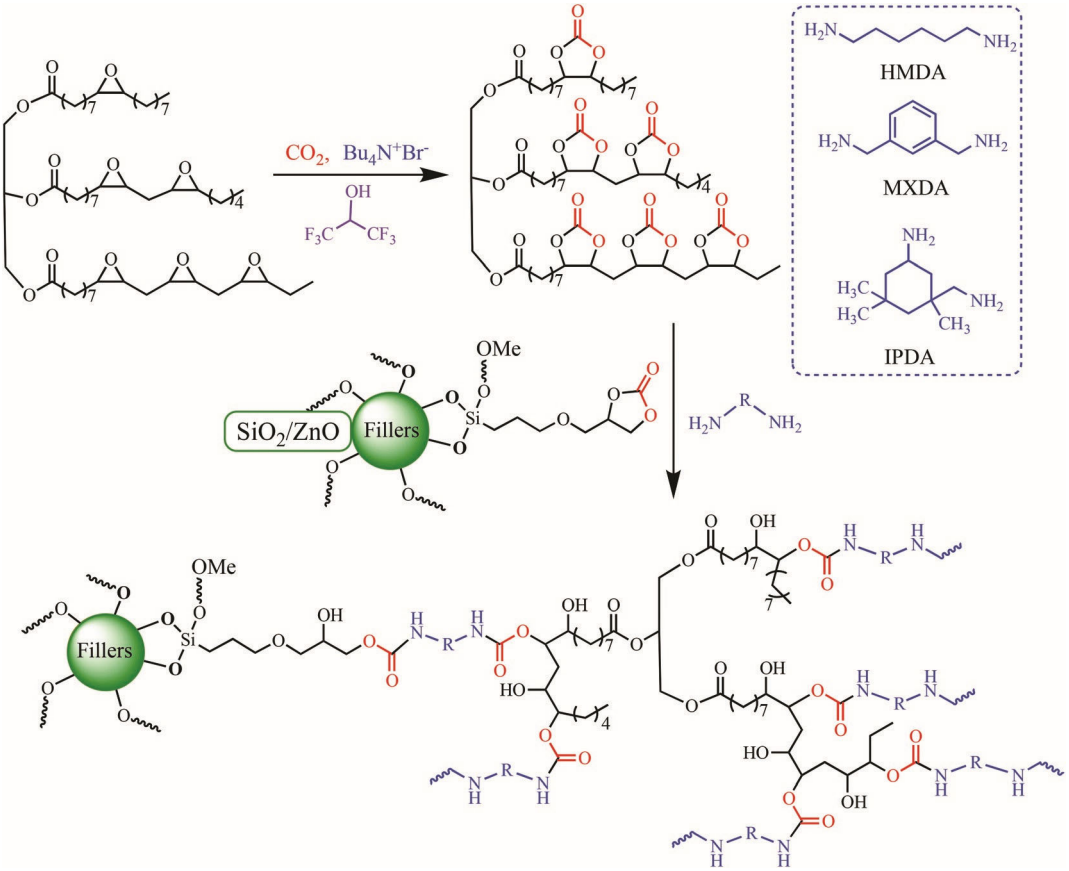

Scheme 1 Synthesis of bio-based nanocomposite thermoset poly(hydroxyurethane) glues for metal sticking (aluminum and/or stainless-steel).

In this contribution, we design novel solvent-free nanocomposite thermoset PHU glues with diversified mechanical strength, limited water uptake, and high bonding strength for various metals (aluminum – Al and stainless steel – SS). The solvent-free PHU glues were prepared from multicyclic carbonates derived

Published in : Polymer Chemistry (2018), vol. 9, issue 19, pp. 2650-2659
doi.org/10.1039/c8py00281a
Status : Postprint (Author's version)

from soybean oil and various amines (aliphatic, cycloaliphatic and aromatic). The cyclocarbonated vegetable oil has been selected not only to confer a sustainable character to the final PHU glue but also to limit its water uptake and to prevent its water induced delamination from the surface as the result of the hydrophobicity of the fatty acid aliphatic chain of the triglyceride. No PDMS is required here in the formulation. All bio-based PHUs were reinforced by introducing cyclic carbonate functional silica (CC-SiO_2) or ZnO (CC-ZnO) fillers that increase the thermo-mechanical properties and the adhesive performances of PHU thermosets (Scheme 1). As vegetable oils are typically composed of mixtures of triglycerides with various chain length (up to 18 C atoms), we determine the optimal formulations by rheological studies prior to evaluating water swelling, contact angle, and thermo-mechanical performances of neat and nanocomposite PHU thermosets. The ability of PHUs to glue Al substrates is evaluated by ASTM standardized crosscut adhesion and MEK double rub tests. This work then investigates the influence of the PHU formulation reinforced by CC-SiO_2 or CC-ZnO fillers on the adhesion performances by lap shear measurements on Al and SS substrates.

Experimental

Materials

Epoxidised soybean oil (ESBO) was kindly donated by Vandeputte Oleochemicals (Belgium). Tetrabutylammonium bromide (TBABr, >99%), 3-(glycidoxypropyl)trimethoxysilane (GPTMS, ≥98%), hexamethylenediamine (HMDA), m-xylylenediamine (MXDA) and isophorone diamine (IPDA) were purchased from Aldrich. Carbon dioxide (CO_2, N48) was supplied by Air Liquid. Hexafluoroisopropanol was purchased from Fluorochem. ZnO®20 nanoparticles (specific surface area of 15–45 $m^2\,g^{-1}$) were received from Umicore, Belgium. CAB-O-SIL®EH5 (specific surface area of 380 $m^2\,g^{-1}$) was received from Cabot. All chemicals were used as received without any purification. Al-2024-T3 substrates were received from SONACA and 316-stainless steel (AK Steel) was kindly provided by the Mechanical Department of ULiege.

Carbonated soybean oil (CSBO),[18] 4-((3-(trimethoxysilyl) propoxy)methyl)-1,3-dioxolan-2-one and cyclic carbonate functional fillers (1.33 cyclic carbonate per nm^2 for CAB-O-SIL EH5 and 0.63 cyclic carbonate per nm^2 for ZnO) were synthesized according to our previously optimized procedures.[42,43]

Characterization studies

Fourier transform infrared spectra (FTIR) measurements. FTIR measurements were carried out on a Nicolet IS5 spectrometer (Thermo Fisher Scientific) equipped with a diamond attenuated transmission reflectance (ATR) device. 32 scans were recorded for each sample over the range of 4000–500 cm^{-1} with a normal resolution of 4 cm^{-1} and spectra were analysed with ONIUM™ software.

Differential scanning calorimetry (DSC). This analysis was performed on a Q1000 TA Instruments calorimeter using standard aluminium pans, calibrated with indium and nitrogen as purge gas. The samples were analysed at a heating rate of 10 °C min^{-1} over a temperature range from −80 °C to 200 °C under a N_2 atmosphere.

Published in : Polymer Chemistry (2018), vol. 9, issue 19, pp. 2650-2659
doi.org/10.1039/c8py00281a
Status : Postprint (Author's version)

Thermogravimetric analysis (TGA). This was performed using a Q500 from TA Instruments system. The thermal degradation of PHUs was measured at a heating rate of 20 °C min^{-1} over the temperature range of 0–700 °C under a nitrogen atmosphere.

Rheology. The curing kinetics of PHU formulations was carried out on an ARES (Advanced Rheometric Expansion System) Rheometric scientific rheometer, equipped with two parallel plate geometries at a frequency of 1 Hz, a strain of 1%, and the measurements were carried out at 100 °C. The evolution of storage, loss modulus and tan δ were monitored as a function of time.

Tensile properties. These were determined at 298 K using an Instron 5594 tensile machine at a speed of 10 mm min^{-1} with a load capacity of 10 000 N. E-Modulus, tensile strength and elongation at break were estimated by the average values of at least 6 repeated PHU samples. Free-standing dog bone shaped reinforced PHU samples were prepared using Teflon molds with the following dimensions: length 3 cm, length of narrow fraction 1 cm, width 0.5 cm, width of narrow fraction 0.2 cm and thickness 0.05 cm.

Water swelling. Water swelling of PHU samples was evaluated using water content and absorption measurements at room temperature for free-standing films following a procedure reported elsewhere.[19,42] PHU samples with dimensions of 0.5 cm (l) × 0.5 cm (t) × 0.5 cm (w) (0.125 cm^3) were immersed in 10 mL Milli-Q water at room temperature. The water uptake was measured until the weight of the swollen samples remains constant. The time evolution of the equilibrium water content (EWC) and equilibrium water absorption (EWA) was estimated using eqn (1) and (2). After swelling measurements, all samples were dried in an oven at 70 °C for 24 h and the gel content was measured using eqn (3):

$$EWC(\%) = \left(\frac{W_s - W_d}{W_d}\right) \times 100 \quad (1)$$

$$EWA(\%) = \left(\frac{W_s - W_d}{W_s}\right) \times 100 \quad (2)$$

$$GC(\%) = \left(\frac{W_f}{W_i}\right) \times 100 \quad (3)$$

where W_s is the weight of the swollen sample, W_d is the weight of the dried sample, W_i is the initial weight and W_f is the final weight of the dried sample.

Water contact angle. These measurements were performed on an OCA-20 apparatus (Dataphysics Instrument GmbH) in the sessile drop configuration by the deposition of a 5 µl droplet of Milli-Q water. The mean contact angle values were determined from at least 5 repeated measurements realized at different locations of each PHU coated Al surface as well as on both sides of the free-standing films.

Scanning electron microscopy (SEM). The morphology of nanocomposite PHU coatings was evaluated using a scanning electron microscopy (SEM, JEOL JSM 840-A) apparatus after metallization of the sample with Pt (30 nm).

Adhesion properties. These properties of PHU coatings were investigated by crosscut adhesion tests according to ASTM D3359 standards. The test consists of making six perpendicular cuts with a distance of 3 mm on a coated Al plate with a sharp razor blade followed by the application of a high-pressure sensitive adhesive tape (Intertape tm 51596-ASTM D3359, Gardco). The tape is then removed by rapid pulling off at an angle of 180 degrees. The quality of the coating was visually estimated by comparison with % of area removed from the total surface.

Published in : Polymer Chemistry (2018), vol. 9, issue 19, pp. 2650-2659
doi.org/10.1039/c8py00281a
Status : Postprint (Author's version)

Solvent resistance. This coatings property was evaluated by the methylethylketone (MEK) double rub test according to the ASTM D4752 standard. The coated Al surface was rubbed with cheesecloth soaked in MEK until failure or breakthrough of the film occurred. Double rubs were repeated for at least 200 movements or until the substrate became visible.

Wet adhesion. This coating property was investigated by a water immersion test. The test consists of making perpendicular cuts with a distance of 10 mm on a coated Al plate with a sharp razor blade followed by immersion in water at room temperature for 5 days. This test is determined by visual appearance of blistering, delamination of the squares at the coating–substrate interface.

Lap-shear adhesion tests. These tests were carried out at 298 K using an Instron 5594 equipped with a 10 000 N load cell at a displacement rate of 2 mm min^{-1}. Aluminum and stainless-steel metal substrates with dimensions of 50 mm (l) × 10 mm (w) × 0.8 mm (t) were used for single lap-shear measurements and the grip length on both sides of test specimens was 25 mm. The tests were performed on at least 5 repeated samples from each type of formulation to determine the average lap-shear strength of adhesives. The lap shear strength was calculated using the following equation:

$$\tau = \frac{P}{A} \tag{4}$$

where τ is the lap shear strength (N mm^{-2} or MPa), P is the force to remove the adhesive or load (N) and A is the over-lapped or gluing area (100 mm^2).

PHU synthesis (representative protocol). Prior to the PHU synthesis, CSBO was degassed by thermal treatment at 60 °C overnight under vacuum. Solvent-free bio-based thermoset PHUs were prepared by mixing equimolar amounts of CSBO (2.0 g, 1.6 mmol, cyclic carbonate mean content/molecule = 6, molar mass approximated to 1250 g mol^{-1})[17,44–47] and diamine (HMDA, 0.5577 g, 4.8 mmol) at 50 °C for 3 minutes under stirring (500 rpm). This mixing time was optimized for obtaining a homogeneous mixture of the components before curing, and that led to the complete conversion of the cyclic carbonate after curing (as assessed by FTIR measurement; Fig. S2†) with the formation of PHU films that did not dissolve in THF or DMF (Fig. S3†). A lower mixing time did not provide a homogeneous mixture before curing (see the ESI for further details, Fig. S3†). The homogeneous viscous formulation was deposited into a Teflon mold to prepare free-standing films (to evaluate swelling measurements and thermo-mechanical properties) or applied on Al-substrates (thickness of 25–30 µm) to measure the contact angle and to perform the crosscut adhesion and MEK double rub tests. Finally, 10 mg of the formulation was applied onto the aluminum and/or stainless steel substrate with a contact area of 100 mm^2 for the evaluation of shear adhesion strength. Then, all samples were cured at 70 °C for 12 h and 100 °C for 4 h in an air circulating oven. Nanocomposite thermoset PHU films based on CSBO and HMDA were prepared following the same protocol but by adding 5 wt% of CC-SiO_2/ZnO fillers (0.1278 g, compared to CSBO and the diamine). The optimal HMDA content in reinforced formulations (0.6135 g or 5.28 mmol and 0.5855 g or 5.04 mmol, respectively, for CC-SiO_2 and CC-ZnO fillers) was determined by identifying the formulation that gives the lowest gel time in rheology (see the Results and discussion section) (Fig. 2).

Reaction of cyclic carbonate functionalized silica (CC-SiO_2) with HMDA. The reaction between CC-SiO_2 (0.2 g) and HMDA (0.96 g) was carried out in THF (3 mL) at 60 °C for 30 min. The solvent was then removed under vacuum and cured at 70 °C for 12 h and 100 °C for 4 h. The product was then washed in MeOH to remove unreacted amine and dried in vacuum at 70 °C for 2 h. The reaction was monitored by FTIR (Fig. S4†).

Published in : Polymer Chemistry (2018), vol. 9, issue 19, pp. 2650-2659
doi.org/10.1039/c8py00281a
Status : Postprint (Author's version)

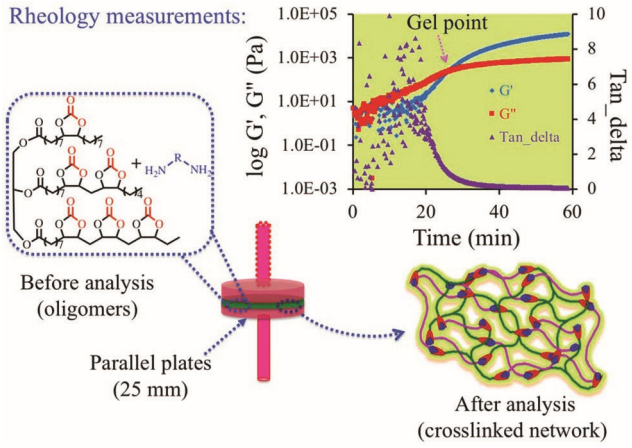

Fig. 1 Curing kinetics and time sweep measurements of CSBO/HMDA formulations by rheology under solvent-free conditions at 100 °C.

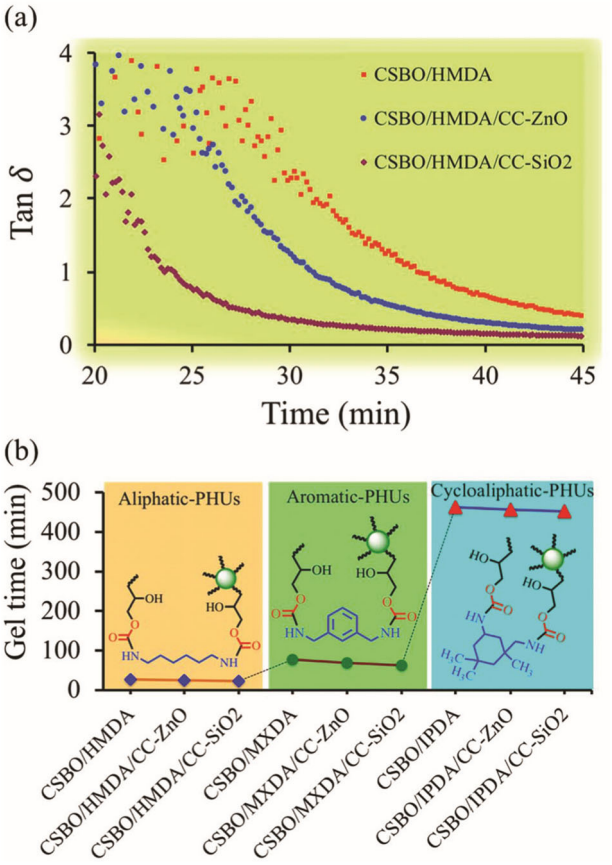

Fig. 2 (a) Evolution of tan delta measured by rheology at 100 °C for 50 min, for neat and reinforced formulations containing 5 wt% of functional (CC-ZnO or CC-SiO_2) fillers and (b) gel time evolution for neat and reinforced formulations produced from HMDA, MXDA, and IPDA using CSBO/diamines 1/3 molar ratio, CSBO/diamines/CC-SiO_2 1/3.3/5 ratio (mol/mol/wt%) and CSBO/diamines/CC-ZnO 1/3.15/5 ratio (mol/ mol/wt%). All formulations were cured under solvent-free conditions at 100 °C and monitored by rheology.

Published in : Polymer Chemistry (2018), vol. 9, issue 19, pp. 2650-2659
doi.org/10.1039/c8py00281a
Status : Postprint (Author's version)

Results and discussion

Determination of gel time by rheology

Rheology properties play an essential role in material selection and processing of adhesives and coatings, where the determination of gel time could be useful for the manufacturing process attributed to the phase transition of formulations throughout the time of curing.[48] Before determining the influence of the nature of the amine (hexamethylenediamine (HMDA), isophorone diamine (IPDA) or m-xylylenediamine (MXDA)) on the curing kinetics of CSBO based PHU thermosets, the optimal CSBO/amine molar ratio was identified by rheology measurements under solvent-free conditions at 100 °C without any catalyst. The molar ratio that gives the shortest gelation time, obtained from the *G"*/*G'* crossover point of the *G"*/*G'* vs. time plot (see Fig. 1 as a typical example) and phase transition due to chemical crosslinking, was selected as the optimal formulation. As a representative example, the evolution of the gelation time for various CSBO/HMDA compositions (PHU-H) is depicted in Fig. S5a† and Table 1. The curing time was the shortest (27 min) for the optimal CSBO/ HMDA molar ratio of 1/3. Similar results were obtained with the other amines (IPDA and MXDA) and this ratio was selected for the following experiments. Table 1 shows that substituting HMDA for the less reactive aromatic amine (MXDA, formulation PHU-M) or cycloaliphatic amine (IPDA, formulation PHU-I) induced an increase in the gelation time from 27 min to 77 min and 463 min, respectively, in line with the decreased reactivity of the amines. FTIR analysis of the starting CSBO and PHU confirms that an almost complete conversion is reached after 50 min of curing at 100 °C, with the disappearance of the typical band of the carbonyl of cyclic carbonate at 1792 cm^{-1} and the appearance of bands of urethane at 1697 cm^{-1} (C==O), 1536 cm^{-1} (N–H), and hydroxyl at 3312 cm^{-1} (Fig. S1†).

The formulations were then reinforced by the addition of 5 wt% of cyclic carbonate functional silica (CC-SiO_2) or ZnO (CC-ZnO) fillers (1.33 or 0.63 cyclic carbonate per nm^2, respectively). Since the presence of terminal cyclic carbonate functional groups on these fillers changes the stoichiometric ratio, compositions were again optimized via rheology by determining the gel time for various CSBO/HMDA molar contents. Irrespective of the filler used, the lowest gel time was observed when a slight excess of amine was used (Fig. S5b and c†). For each formulation (in the investigated composition range), the addition of the functional filler slightly accelerated the curing rate as evidenced by a small reduction in the gel time (Table 1). The presence of the particles also improved the cross-linking density of the PHU-thermosets as confirmed by a reduction of the tan delta values at 45 min (Fig. 2a and Table 1).[49] Indeed, a value of 0.4 was reported for CSBO/HMDA, while lower values of 0.2 for CSBO/HMDA/CC-ZnO and 0.12 for CSBO/HMDA/CC-SiO_2 formulations were measured. This trend might be explained by (i) the higher reactivity of the terminal cyclic carbonates present at the surface of the fillers compared to the internal cyclic carbonates in CSBO and (ii) the extent of crosslinking density of PHUs in the presence of functional fillers.

In order to demonstrate that the cyclic carbonate-functionalized nanoparticles are able to react with the amine, the reaction between bare and/or cyclic carbonate functionalized fillers and amine was performed in THF at 60 °C for 30 minutes followed by curing at 70 °C for 12 h and 100 °C for 4 h. Fillers were then washed with MeOH to remove unreacted amine and dried in vacuum at 70 °C for 2 h. Fig. S4† shows the FT-IR spectra of HMDA, CC-SiO_2, and CC-SiO_2 reacted with HMDA (CC-SiO_2-HMDA). Clearly, the grafting of HMDA to CC-SiO_2 was evidenced by the disappearance of the typical band of the carbonyl of cyclic carbonate at 1792 cm^{-1} and the appearance of the bands of urethane at 1697 cm^{-1} (C==O) and 1536 cm^{-1} (N–H).

Published in : Polymer Chemistry (2018), vol. 9, issue 19, pp. 2650-2659
doi.org/10.1039/c8py00281a
Status : Postprint (Author's version)

Table 1 Formulation, swelling and adhesion properties of (reinforced) CSBO-derived PHU-thermosets

Sample code	Formulation		GT[b] (min)	tan δ[c]	EWC[d] (%)	EWA[e] (%)	GC[f] (%)	CA[g] (0)	Adhesion[h]
	CSBO (mol)/amine (mol)/filler[a] (wt%)								
PHU-H1	CSBO/HMDA	1/3/0	27	0.40	6.8 ± 0.4	7.2 ± 0.5	96.2	95 ± 2	5B
PHU-H2	CSBO/HMDA/CC-SiO_2	1/3.3/5	22	1.12	4.1 ± 0.2	4.3 ± 0.2	98.5	97 ± 1	5B
PHU-H3	CSBO/HMDA/CC-ZnO	1/3.15/5	24	0.20	3.5 ± 0.1	3.6 ± 0.1	98.1	101 ± 2	5B
PHU-M1	CSBO/MXDA	1/3/0	77	0.56	3.8 ± 0.2	4.0 ± 0.1	98.6	103 ± 1	5B
PHU-M2	CSBO/MXDA/CC-SiO_2	1/3.3/5	68	0.15	3.6 ± 0.1	3.7 ± 0.2	98.8	109 ± 2	5B
PHU-M3	CSBO/MXDA/CC-ZnO	1/3.15/5	72	0.29	2.8 ± 0.1	2.9 ± 0.1	98.9	112 ± 1	5B
PHU-I1	CSBO/IPDA	1/3/0	463	0.92	4.5 ± 0.2	4.8 ± 0.1	97.6	99 ± 3	5B
PHU-I2	CSBO/IPDA/CC-SiO_2	1/3.3/5	455	0.63	3.8 ± 0.1	4.5 ± 0.2	98.1	103 ± 2	5B
PHU-I3	CSBO/IPDA/CC-ZnO	1/3.15/5	452	0.75	3.0 ± 0.4	3.1 ± 0.1	96.4	108 ± 1	5B

[a] Optimum molar compositions determined by rheology (Fig. S5 and Fig. 2a, b). [b] GT – gel time (determined by rheology at 100 °C). [c] tan δ values in the plateau region (at 45 min (for PHU-H), at 136 min for (PHU-M) and at 600 min for (PHU-I)). [d] EWC – equilibrium water content. [e] EWA – equilibrium water absorption of free-standing films 0.5 cm (l) × 0.5 cm (t) × 0.5 cm (w) or (0.125 cm^3) for 48 h. [f] GC – gel content. [g] CA – contact angle. [h] Cross-cut adhesion test (performed *via* maintaining a 3 mm space between cuts according to standardised ASTM D3359).

Swelling measurement of free-standing PHU films

Previous studies have shown that the pendant hydroxyl groups of PHUs favoured the interactions with the aluminum substrate by hydrogen bonding.[42] However, they also increase the hydrophilicity and water uptake of PHUs, which might be detrimental for their wet adhesion by inducing delamination of the glue.[42,50,51] The water uptake is therefore a qualitative information regarding the ability of the PHU glue to delaminate or not in an aqueous environment. The water uptake of our bio-based (nanocomposite) PHUs was evaluated on freestanding PHU films by water absorption experiments. In the absence of fillers, all formulations led to PHUs with low equilibrium water absorption (EWA) values ranging from 7.2% for PHU-H to 4.8% for PHU-I and 4.0% for PHU-M (Table 1, Fig. S7 and Fig. S8a†). These values are much lower than the ones measured for PHUs based on small multifunctional cyclic carbonate molecules (TMPTC) and charged with 5 wt% of PDMS (EWA of 57%).[42] These lower water uptake values arise from the hydrophobic nature of CSBO induced by the long aliphatic chain (up to C_{18}) of the triglyceride. Upon addition of 5 wt% of cyclic carbonate functional silica or ZnO fillers, EWA values significantly decreased compared to unfilled PHU thermosets. For all formulations, the reduction in the water uptake is more prominent with ZnO than with SiO_2 fillers (Table 1). For instance, the addition of CC-ZnO to the CSBO/HMDA formulation drastically decreased the EWA value from 7.2% to 3.6%, compared to 4.3% with CC-SiO_2. The decrease in the water absorption of PHU reinforced by fillers may be correlated to the higher crosslinking density of the nanocomposite materials compared to unfilled PHUs. The same trend is noted for the equilibrium water content (EWC, Table 1). The gel content of the different PHU films is rather similar and high, between 96.2 and 98.9%, with no significant difference between the different formulations (Table 1). This observation indicates a highly crosslinked material in all cases.

Contact angle measurements of PHU coatings

The hydrophobic nature of (reinforced) PHU thermosets was further confirmed by contact angle measurement of PHU coatings on aluminium (thickness: 25–30 µm). Free-flowing solvent-free viscous PHU

Published in : Polymer Chemistry (2018), vol. 9, issue 19, pp. 2650-2659
doi.org/10.1039/c8py00281a
Status : Postprint (Author's version)

formulations prepared by mixing CSBO with diamines for 3 min at 50 °C were first deposited onto the metal surface for coating and into Teflon molds for freestanding films (thickness: 500 µm) *via* a bar-coater. After curing at 70 °C for 12 h and 100 °C for 4 h, the water contact angle of PHU coatings was measured. The coatings produced from unfilled PHU formulations exhibit contact angle values ranging from 95 ± 2° for PHU-H1 to 99 ± 3° for PHU-I1 and 103 ± 1° for PHU-M1 (Fig. S8b† and Table 1). The coatings are therefore hydrophobic, as expected from the hydrophobic formulation. PHU-M1 prepared from the aromatic diamine (MXDA) presents a higher hydrophobicity. The addition of 5 wt% of CC-SiO_2 or CC-ZnO to CSBO/diamine formulations slightly increased the hydrophobicity of coatings with contact angle values up to 112° for PHU prepared from MXDA (PHU-M3, Table 1), which can be due to an increase in the surface roughness in the presence of fillers as evidenced by SEM (Fig. S6†). Additionally, contact angle measurements were also performed on both sides of free-standing films and similar values were obtained which suggests the homogeneity of the filler dispersion. Again, the CC-ZnO filler has the highest impact on the coating hydrophobicity, in line with the water absorption experiments (Fig. S7 and Fig. S8,† respectively).

Thermal properties

The thermal stability of bio-based thermoset PHU nanocomposite materials was evaluated by thermogravimetric analysis (TGA) (Fig. S9†). The temperatures at 5% degradation ($T_{d\,5\%}$) are shown in Table 2 and Fig. 3a.

Table 2 Thermal and mechanical properties of bio- and CO_2-sourced neat and nanocomposite thermoset PHU glues

Sample code	T_g [a] (°C)	$T_{d\,5\%}$ [b]	E [c] (MPa)	σ_{Yield} [d] (MPa)	ε_{break} [e] (MPa)
PHU-H1	9.9	246.8	65 ± 6	6.1 ± 0.3	308 ± 3
PHU-H2	9.6	252.1	80 ± 9	5.4 ± 0.6	262 ± 9
PHU-H3	13.3	257.3	86 ± 8	3.7 ± 0.2	194 ± 2
PHU-M1	21.3	260.5	94 ± 3	7.5 ± 0.3	227 ± 3
PHU-M2	21.5	270.4	107 ± 5	6.4 ± 0.4	220 ± 9
PHU-M3	24.6	277.3	132 ± 12	6.3 ± 0.2	205 ± 2
PHU-I1	26.0	249.5	161 ± 5	8.3 ± 0.2	177 ± 3
PHU-I2	27.2	254.2	200 ± 13	7.4 ± 0.5	151 ± 7
PHU-I3	27.9	259.8	215 ± 7	5.3 ± 0.3	26 ± 1

Bio-based PHU thermoset glues and analogous PHUs reinforced with 5 wt% CC-SiO_2 or CC-ZnO fillers. [a] Determined by DSC, heating rate: 10 °C min^{-1}. [b] Determined by TGA, heating rate: 20 °C min^{-1}. [c] Young's modulus. [d] Tensile strength. [e] Elongation at break (PHU-H: aliphatic, PHU-M: aromatic and PHU-I: cyclic aliphatic thermosets) [PHU-H1, PHU-M1 and PHU-I1: unfilled PHUs, PHU-H2, PHU-M2 and PHU-I2: PHUs reinforced with 5 wt% CC-SiO_2; PHU-H3, PHU-M3 and PHU-I3: PHUs reinforced with 5 wt% CC-ZnO].

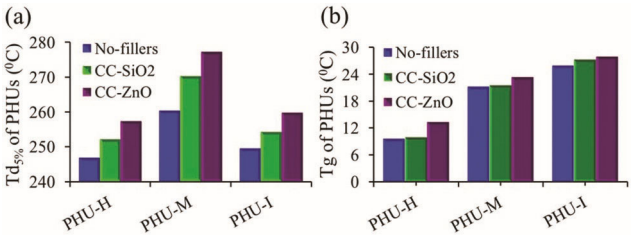

Fig. 3 Evolution of the thermal stability at 5% degradation ($T_{d\,5\%}$) (a) and glass transition temperature (T_g) (b) as a function of the amine structure (H, aliphatic, I, cycloaliphatic and M, aromatic) of the PHU formulation and the filler (CC-SiO_2 or CC-ZnO) (PHU-H: aliphatic, PHU-M: aromatic and PHU-I: cyclic aliphatic thermosets).

Published in : Polymer Chemistry (2018), vol. 9, issue 19, pp. 2650-2659
doi.org/10.1039/c8py00281a
Status : Postprint (Author's version)

In the absence of fillers, polymers started to decompose above 246 °C as attested by $T_{d\ 5\%}$ values of 246.8 °C, 249.5 °C and 270.4 °C for PHUs synthesized, respectively, from CSBO/HMDA, CSBO/IPDA and CSBO/MXDA formulations. The thermal stability was in the same range for the formulations that were reinforced by 5 wt% CC-SiO_2. The addition of functional CC-ZnO fillers has a more pronounced stabilization effect with $T_{d\ 5\%}$ values that increased to 257.3 °C, 259.8 °C and 277.3 °C for CSBO/HMDA, CSBO/IPDA and CSBO/MXDA formulations. Although the thermal stability varied slightly with the nature of the amines, the positive impact of the fillers on this stability probably results from the improved cross-linking of the thermoset PHUs that limits the diffusion of gases during the thermal degradation.

The glass transition temperature (T_g) of each PHU was determined by differential scanning calorimetry (DSC) analysis (Table 2, Fig. 3b and Fig. S10†). PHU-H and reinforced PHU-H exhibit a T_g in the range of 9.9–13.3 °C, PHU-M and reinforced PHU-M in the range of 21.3–24.6 °C, and PHU-I and reinforced PHU-I between 26 and 27.9 °C. As expected, the evolution of this T_g is mainly governed by the nature of the amine and increased in the order aliphatic < aromatic < cycloaliphatic diamine, in line with the expected increased rigidity order of the corresponding polymers.

Mechanical properties

The influence of the amine structure and of CC-silica/ZnO fillers on the mechanical properties of PHU thermosets was investigated by conventional tensile tests (Fig. 4a). All results are summarized in Table 2 and Fig. 4b. Young's modulus of PHU increased with the PHU rigidity, thus with the nature of the diamine used, *i.e*. for HMDA ($E_{PHU\text{-}H1}$ = 65 MPa) < MXDA ($E_{PHU\text{-}M1}$ = 94 MPa) < IPDA ($E_{PHU\text{-}I1}$ = 161 MPa), whereas the elongation at break decreased with the PHU rigidity, i.e. for HMDA ($\varepsilon_{PHU\text{-}H1}$ = 308%) > MXDA ($\varepsilon_{PHU\text{-}M1}$ = 227%) > IPDA ($\varepsilon_{PHU\text{-}I1}$ = 177%). For all formulations, the addition of SiO_2 or ZnO particles increased Young's modulus and decreased the elongation at break, as the result of extent of crosslinking density and the formation of a denser network in the presence of the functional particles. Formulations with IPDA and CC-ZnO particles became very brittle, clearly highlighting a transition from elastic (reinforced) PHUs produced from HMDA to rigid and brittle (reinforced) materials by replacing the aliphatic by the cycloaliphatic diamines.

Adhesive performances

Prior to determining the shear strength of the PHU glues, the adhesion performances of 25–30 µm thick coatings deposited on the bare Al surface were qualitatively investigated by the standardized ASTM D3359 cross-cut test (Table 1) performed by maintaining a 3 mm space between the cuts. Whatever the PHU formulation, the edges of the cuts were completely smooth and none of the squares of the coatings were removed after tape removal. All PHU coatings were classified as 5B-0%. Such high adhesion properties make the (reinforced) biobased thermoset PHUs good candidates for designing high performance glues. The resistance of coatings against solvents was also investigated by the MEK double rub test in line with ASTM D4752 standards. After 200 double rubs, no visible surface defects and/or wiping off of the coatings from the surface could be detected, confirming the excellent adhesion of all PHU formulations onto the Al substrate. Additionally, the wet adhesion performance of thermosets was evaluated by immersing coatings in water at room temperature for 5 days. Fig. 5 shows that unfilled PHU coatings were peeled off after immersion for 5 days. In contrast, the nanocomposite coatings were stable under the same conditions, and no delamination was observed. This study illustrates that reinforced functional fillers significantly improve the film stability in wet environments, in agreement with the water uptake results.

Published in : Polymer Chemistry (2018), vol. 9, issue 19, pp. 2650-2659
doi.org/10.1039/c8py00281a
Status : Postprint (Author's version)

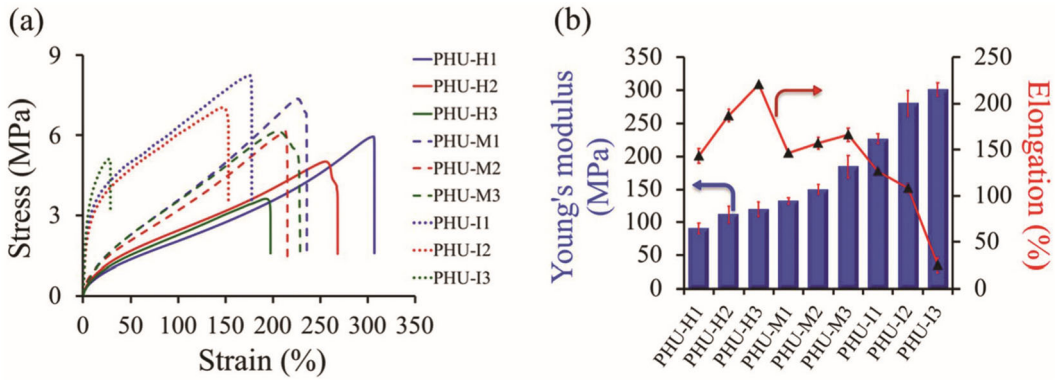

Fig. 4 Evolution of the mechanical properties of PHUs. (a) Stress vs. strain and (b) Young's modulus & elongation (%) at break vs. evolution for the various CSBO/diamine formulations (neat or reinforced with 5 wt% CC-SiO_2 or CC-ZnO) (PHU-H: aliphatic, PHU-M: aromatic and PHU-I: cyclic aliphatic thermosets).

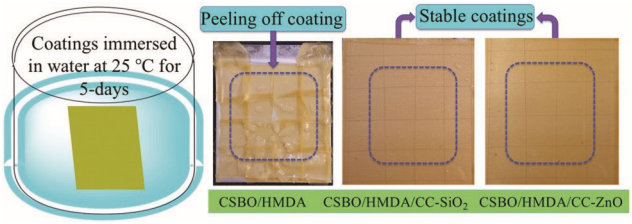

Fig. 5 Evolution of wet adhesion of PHU and analogous nanocomposite thermoset coatings immersed in water at 25 °C for 5 days. The coatings were manually cut into squares (thus, distance of 10 mm between cuts) to visualize peeling off of coating.

Then, the shear adhesion performances of the bio-based nanocomposite PHU glues were evaluated for sticking aluminum to aluminum (Al–Al) (Fig. 6a and b) and stainless steel to stainless steel (SS–SS) substrates (Fig. 6c and 6d and Table S1†). Adhesion values were quantified by lap shear tests using eqn (4). For Al substrates, the lap shear strength for bare PHU adhesives varied from about 6.5 MPa for PHU-H and PHU-M to 3.7 MPa for PHU-I. The lowest adhesive performance of CSBO/IPDA PHU glues was related to the high T_g values and the brittleness of the crosslinked material that are detrimental to the adhesion. Indeed, the presence of flexible/soft segments in conventional PUs or PHUs is most often required for high adhesion performances.[41,52] The addition of functional (CC-SiO_2 or CC-ZnO) fillers increased the adhesion strength of PHU due to the extent of crosslinking. The effect is more pronounced with CC-ZnO for PHU-H with lap shear strength values up to 11.3 MPa, corresponding to 173% increase compared to bare PHU-H. This improvement is explained by a higher crosslinking density of reinforced PHUs that increased the mechanical strength without sacrificing elongation at break of the glue. This trend is further confirmed for PHU-M and PHU-I with a shear strength that increased by 117% (up to 7.5 MPa, PHU-M3) and 160% (up to 5.9 MPa, PHU-I3), respectively, upon addition of 5 wt% of CC-ZnO. All PHU glues underwent cohesive failure (CF) with the exception of reinforced PHU-I that showed an adhesive failure (AF) mode as the result of too rigid crosslinked materials that disfavoured adhesive–metal substrate interaction. Interestingly, nanocomposite PHU glues also showed promising adhesion performances to stainless steel (SS) with adhesion strength up to 10.1 MPa for PHU-H reinforced by 5 wt% CC-ZnO. As observed for Al–Al sticking, reinforced formulations made of CSBO and MXDA or IPDA gave glues with significantly lower adhesion performances as attested by shear strength values of 6.9 and 4.6 MPa, respectively.

Published in : Polymer Chemistry (2018), vol. 9, issue 19, pp. 2650-2659
doi.org/10.1039/c8py00281a
Status : Postprint (Author's version)

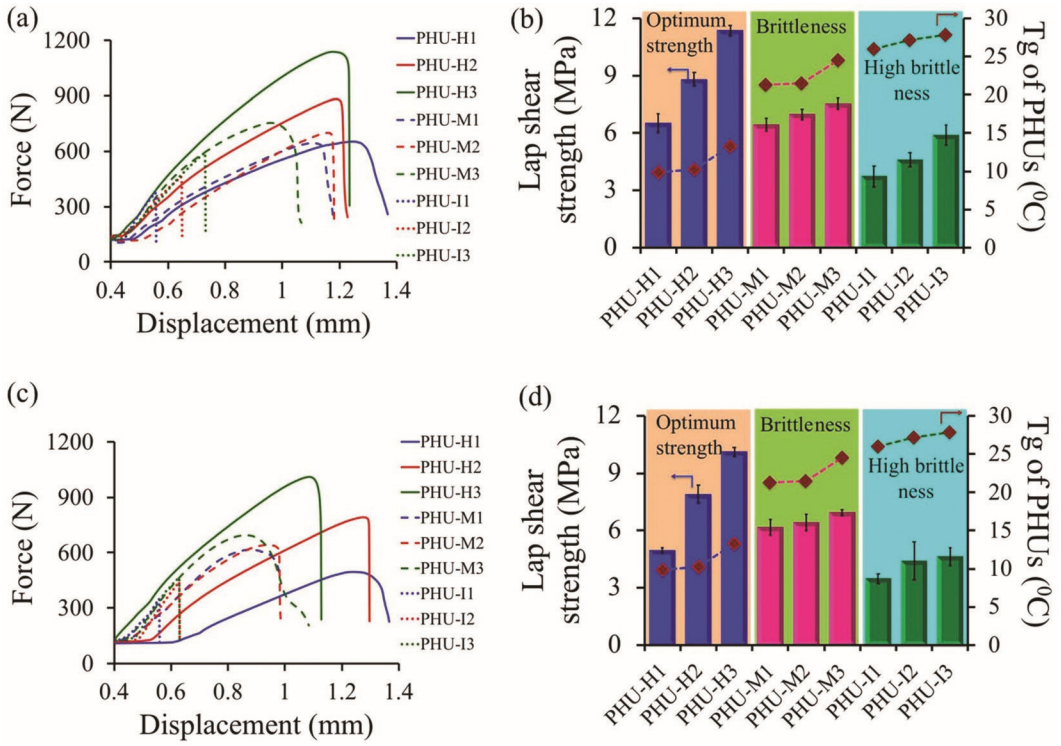

Fig. 6 Influence of the amine structure (H-HMDA, M-MXDA and I-IPDA) and filler (CC-SiO_2 or CC-ZnO) on the adhesive performances of PHUs for Al–Al (a and b) and SS–SS (c and d) substrate sticking (PHU-H: aliphatic, PHU-M: aromatic and PHU-I: cyclic aliphatic thermosets). Product codes and compositions are summarized in Table 1.

The bio-based PHU with the best adhesion performance (PHU-H3) was then benchmarked against commercial polyurethane (PU) adhesives (Teromix-6700 and Araldite®2000) and recently reported PHU adhesives (thus, PHU(M-1):[41] TMPTC/EDR-148, PHU-5C:[42] TMPTC/HMDA/PDMS/C-GPTMS-ZnO). All adhesives are tested on Al under identical conditions, thus with the same amount of glue (10 mg), on the same area (100 mm^2) and under identical curing conditions (time and temperature) (70 °C for 12 h and 4 h at 100 °C and/ or 48 h at 25 °C). The results are shown in Fig. 7 and Table S2 (ESI†). The commercial PU adhesives exhibited the highest performance when cured at 25 °C for 48 h [Araldite up to 21.7 MPa and Teromix up to 12.5 MPa] whereas PHU adhesives showed a low lap shear strength (PHU(M-1),[41] PHU-5C,[42] PHU-H3: 1.9, 3.3 and 2.2 MPa, respectively).

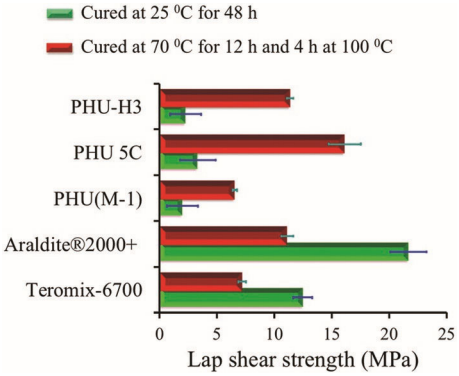

Fig. 7 Adhesive performance of bio-based nanocomposite thermoset PHU glue (PHU-H3) benchmarked against commercial PU (Teromix6700 and Araldite®2000+) glues, and recently reported PHU adhesives (PHU(M-1)[41] and PHU-5C[42]), tested on aluminum substrates.

This poor adhesion performance for PHUs is the result of their too slow curing due to the low reactivity of cyclic carbonates towards amines at 25 °C. On the other hand, the bio-based glue (PHU-H3) competes with commercial glues (at least with Teromix) when cured under our optimized conditions (70 °C for 12 h and 100 °C for 4 h) with a shear strength of 11.3 MPa. Although the adhesion performance is slightly lower compared to our previous PHU-5C[42] and to Araldite, PHU-H3 is formulated from a sustainable bio-sourced cyclic carbonate without any solvent, does not contain any PDMS and does not involve isocyanate chemistry. This benchmarking clearly highlights that well-designed PHU glues can afford a realistic alternative to conventional PU glues. These sustainable high-performance bio-nanocomposite PHU adhesives are therefore promising for applications that are compatible with a thermal curing.

Conclusion

We reported on the preparation of novel bio-based nanocomposite poly(hydroxyurethane) thermoset glues for aluminum and stainless-steel substrates. These glues were formulated by the polyaddition of cyclic carbonate bearing vegetable oil (soybean oil) with (cyclo) aliphatic or aromatic diamines under solvent-free conditions. Various formulations reinforced with cyclic carbonate functionalized SiO_2 or ZnO fillers were also designed. Through swelling, contact angle measurements and wet adhesion, we demonstrated that the coating hydrophobicity induced by the long fatty ester chains (up to C_{18}) of soybean oil prevented water swelling of the thermoset PHU films and coating delamination from the surface when immersed in water. All PHU coatings presented good adhesion to Al according to the ASTM D3359 standard crosscut adhesion test and showed excellent mechanical properties and thermal stabilities (up to 277 °C). Formulations composed of aliphatic hexamethylene diamine and CSBO containing 5 wt% of functional ZnO provided reinforced PHU biobased glues offering the best compromise between extent of crosslinking, high thermal and mechanical properties, and the highest lap-shear adhesion strength for Al–Al and/or SS–SS substrates with shear strengths up to 11.3 MPa and 10.1 MPa, respectively. The maximum shear adhesion strength for Al was benchmarked against commercial polyurethane glues (Teromix-6700 and Araldite®2000) and recently reported non-biosourced PHUs (PHU(M-1)[41] and PHU-5C[42]). This study has shown that biobased nanocomposite PHU thermosets represent attractive sustainable alternatives to conventional glues made of toxic formulations containing isocyanates. Current works investigate routes to cure the formulations at room temperature, while still improving the PHU adhesion strength.

Conflicts of interest

The authors declare no conflict of interest.

Acknowledgements

The authors of Liège acknowledge the "Region Wallonne" in the frame of the Flycoat and CO_2 Green projects, the "Belgian Science Policy" in the frame of the "Interuniversity Attraction Poles Programme (IAP VII/5) – Functional Supramolecular Systems" and the "Fonds National pour la Recherche Scientifique" (F.R.S.-FNRS) for financial support. C. D. is Research Director of F.R.S.-FNRS.

Published in : Polymer Chemistry (2018), vol. 9, issue 19, pp. 2650-2659
doi.org/10.1039/c8py00281a
Status : Postprint (Author's version)

Notes and references

1 O. Bayer, Angew. Chem., 1947, 59, 257–272.

2 R. Auvergne, S. Caillol, G. David, B. Boutevin and J. P. Pascault, Chem. Rev., 2014, 114, 1082–1115.

3 H.-W. Engels, H.-G. Pirkl, R. Albers, R. W. Albach, J. Krause, A. Hoffmann, H. Casselmann and J. Dormish, Angew. Chem., Int. Ed., 2013, 52, 9422–9441.

4 C. D. Diakoumakos and D. L. Kotzev, Macromol. Symp., 2004, 216, 37–46.

5 T. Thomson, Polyurethanes as Specialty Chemicals Principles and Applications, CRC Press, 2005.

6 O. Kreye, H. Mutlu and M. A. R. Meier, Green Chem., 2013, 15, 1431–1455.

7 S. M. Tarlo and G. M. Liss, Appl. Occup. Environ. Hyg., 2002, 17, 902–908.

8 M. G. Ott, W. F. Diller and A. T. Jolly, Crit. Rev. Toxicol., 2003, 33, 1–59.

9 S. Merenyi, Reach Regul. No. 1907/2006 Consol. version (June 2012) with an Introd. Futur. Prospect. regarding area Chem. Legis., vol. 2, GRIN Verlag,2012.

10 W. H. Carothers, Chem. Rev., 1931, 8, 353–426.

11 T. Sakai, N. Kihara and T. Endo, Macromolecules, 1995, 28, 4701–4706.

12 N. Kihara and T. Endo, J. Polym. Sci., Part A: Polym. Chem., 1993, 31, 2765–2773.

13 H. Tomita, F. Sanda and T. Endo, J. Polym. Sci., Part A: Polym. Chem., 2001, 39, 851–859.

14 L. Maisonneuve, O. Lamarzelle, E. Rix, E. Grau and H. Cramail, Chem. Rev., 2015, 115, 12407–12439.

15 V. Besse, F. Camara, F. Méchin, E. Fleury, S. Caillol, J.-P. Pascault and B. Boutevin, Eur. Polym. J., 2015, 71, 1–11.

16 M. Alves, R. Mereau, B. Grignard, C. Detrembleur, C. Jerome and T. Tassaing, RSC Adv., 2016, 6, 36327–36335.

17 M. Alves, B. Grignard, S. Gennen, C. Detrembleur, C. Jerome and T. Tassaing, RSC Adv., 2015, 5, 53629–53636.

18 L. Poussard, J. Mariage, B. Grignard, C. Detrembleur, Jérôme, C. Calberg, B. Heinrichs, J. De Winter, P. Gerbaux, J.-M. Raquez, L. Bonnaud and P. Dubois, Macromolecules, 2016, 49, 2162–2171.

19 S. Gennen, B. Grignard, J.-M. Thomassin, B. Gilbert, B. Vertruyen, C. Jerome and C. Detrembleur, Eur. Polym. J., 2016, 84, 849–862.

20 B. Grignard, J.-M. Thomassin, S. Gennen, L. Poussard, L. Bonnaud, J.-M. Raquez, P. Dubois, M.-P. Tran, C. B. Park, C. Jerome and C. Detrembleur, Green Chem., 2016, 18, 2206–2215.

21 S. Gennen, B. Grignard, T. Tassaing, C. Jérôme and C. Detrembleur, Angew. Chem., Int. Ed., 2017, 56, 10394– 10398.

22 M. Alves, B. Grignard, S. Gennen, R. Mereau, Detrembleur, C. Jerome and T. Tassaing, Catal. Sci. Technol., 2015, 5, 4636–4643.

23 H. Tomita, F. Sanda and T. Endo, J. Polym. Sci., Part A: Polym. Chem., 2001, 39, 3678–3685.

24 P. Anastas and N. Eghbali, Chem. Soc. Rev., 2010, 39, 301–312.

25 M. Bähr and R. Mülhaupt, Green Chem., 2012, 14, 483–489.

26 Javni, D. P. Hong and Z. S. Petrović, J. Appl. Polym. Sci., 2008, 108, 3867–3875.

27 Lee and Y. Deng, Eur. Polym. J., 2015, 63, 67–73.

28 O. Figovsky, A. Leykin and L. Shapovalov, Altern. Energy Ecol., 2016, 4, 95–108.

29 M. S. Kathalewar, P. B. Joshi, A. S. Sabnis and V. C. Malshe, RSC Adv., 2013, 3, 4110–4129.

30 M. Blain, L. Jean-Gérard, R. Auvergne, D. Benazet, S. Caillol and B. Andrioletti, Green Chem., 2014, 16, 4286–4291.

31 V. Besse, R. Auvergne, S. Carlotti, G. Boutevin, B. Otazaghine, S. Caillol, J.-P. Pascault and B. Boutevin, React. Funct. Polym., 2013, 73, 588–594.

32 J. Guan, Y. Song, Y. Lin, X. Yin, M. Zuo, Y. Zhao, X. Tao and Q. Zheng, Ind. Eng. Chem. Res., 2011, 50, 6517–6527.

33 S. Samanta, S. Selvakumar, J. Bahr, D. S. Wickramaratne, M. Sibi and B. J. Chisholm, ACS Sustainable Chem. Eng., 2016, 4, 6551–6561.

34 K. M. F. Rossi de Aguiar, U. Specht, J. F. Maass, D. Salz, C. A. Picon, P.-L. M. Noeske, K. Rischka and U. P. Rodrigues-Filho, RSC Adv., 2016, 6, 47203–47211.

35 M. Tryznowski, A. Świderska, T. Gołofit and Z. ŻołekTryznowska, RSC Adv., 2017, 7, 30385–30391.

36 Z. Li, Y. Zhao, S. Yan, X. Wang, M. Kang, J. Wang and H. Xiang, Catal. Lett., 2008, 123, 246–251.

37 L. Annunziata, A. K. Diallo, S. Fouquay, G. Michaud, F. Simon, J.-M. Brusson, J.-F. Carpentier and S. M. Guillaume, Green Chem., 2014, 16, 1947–1956.

38 B. Ochiai, Y. Satoh and T. Endo, J. Polym. Sci., Part A: Polym. Chem., 2009, 47, 4629–4635.

39 M. V. Zabalov, R. P. Tiger and A. A. Berlin, Dokl. Chem., 2012, 441, 355–360.

40 E. K. Leitsch, W. H. Heath and J. M. Torkelson, Int. J. Adhes. Adhes., 2016, 64, 1–8.

41 Cornille, G. Michaud, F. Simon, S. Fouquay, R. Auvergne, B. Boutevin and S. Caillol, Eur. Polym. J., 2016, 84, 404–420.

42 S. Panchireddy, J.-M. Thomassin, B. Grignard, C. Damblon, A. Tatton, C. Jerome and C. Detrembleur, Polym. Chem., 2017, 8, 5897–5909.

43 B. Grignard, C. Calberg, C. Jérôme, W. Wang, S. Howdle and C. Detrembleur, Chem. Commun., 2008, 44, 5803–5805.

44 G. Karmakar and P. Ghosh, ACS Sustainable Chem. Eng., 2016, 4, 775–781.

45 Ghosal, O. U. Rahman and S. Ahmad, Ind. Eng. Chem. Res., 2015, 54, 12770–12787.

46 M. Sacristán, J. C. Ronda, M. Galià and V. Cádiz, Biomacromolecules, 2009, 10, 2678–2685.

47 C. Zhang, Y. Xia, R. Chen, S. Huh, P. A. Johnston and M. R. Kessler, Green Chem., 2013, 15, 1477–1484.

48 Z. Wu, W. Cai, R. Chen and J. Qu, Prog. Org. Coat., 2018, 119, 116–122.

49 H. Sardon, L. Irusta, P. Santamaría and M. J. Fernández Berridi, J. Polym. Res., 2012, 19, 9956.

50 L. B. Manfredi, A. N. Fraga and A. Vázquez, J. Appl. Polym. Sci., 2006, 102, 588–597.

51 Merdas, A. Tcharkhtchi, F. Thominette, J. Verdu, K. Dean and W. Cook, Polymer, 2002, 43, 4619–4625.

52 K. Nakamae, T. Nishino, S. Asaoka and Sudaryanto, Int. J. Adhes. Adhes., 1996, 16, 233–239.